THE JOURNAL OF PHYSICAL CHEMISTRY C

Article

pubs.acs.org/JPCC

Molecule–Substrate Coupling between Metal Phthalocyanines and Epitaxial Graphene Grown on Ru(0001) and Pt(111)

K. Yang, W. D. Xiao, Y. H. Jiang, H. G. Zhang, L. W. Liu, J. H. Mao, H. T. Zhou, S. X. Du, and H.-J. Gao*

Beijing National Laboratory of Condensed Matter Physics, Institute of Physics, Chinese Academy of Sciences, Beijing 100190, China

ABSTRACT: Self-assembly of metal phthalocyanine (MPc) molecules on monolayer graphene (MG) epitaxially grown on Ru(0001) and Pt(111) is investigated by means of low-temperature scanning tunneling microscopy. At low coverage, dispersive single molecules, dispersive molecular chains, and small patches of Kagome lattice are observed for iron phthalocyanine (FePc), manganese phthalocyanine (MnPc), nickel phthalocyanine (NiPc), and phthalocyanine (H_2Pc) on MG/Ru(0001). In contrast, although MG/Pt(111) exhibits various domains with different moiré patterns and corrugations, FePc molecules always form densely packed two-dimensional islands with a square lattice on MG/Pt(111) at submonolayer coverage. The different self-assembling behaviors of MPc molecules on MG/Ru(0001) and MG/Pt(111) originate from a subtle balance between molecule–molecule and molecule–substrate interactions tuned by central metal ions of the MPc molecules and the metal substrates.

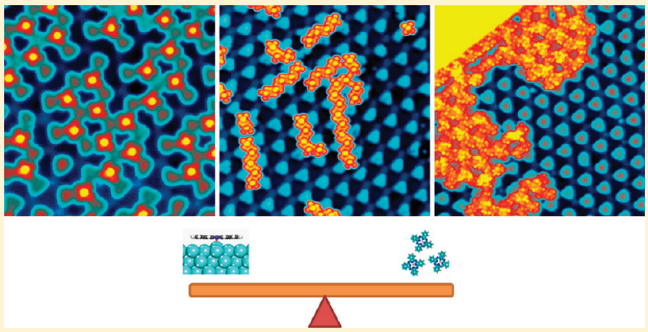

INTRODUCTION

Graphene, a single layer of sp^2-bonded carbon atoms with a honeycomb lattice, has been attracting great interest because of its outstanding physical properties[1−3] and potential applications.[4−7] To fulfill the requirement of the forthcoming graphene-based technology, it is vital to incorporate other materials into graphene and understand their interfacial structures and coupling. It has been found that the electronic structures and transport properties of graphene can be tuned by the metal substrates that the graphene sheets were epitaxially grown on due to different graphene–substrate interactions.[8] For instance, the strong interaction between graphene sheets and Ru(0001) and Ni(111) substrates results in a dramatic modification of the density of states (DOS) near the Fermi level[9,10] and a n-doped feature of the thermoelectrical property,[8] whereas the graphene sheets grown on Pt(111) preserve the intrinsic "V"-shaped DOS of free-standing graphene because of a weak graphene–substrate interaction.[11] Adsorption of organic molecules on graphene is also an issue of special importance. Because of charge transfer between molecular adsorbates and graphene, the graphene sheets are shown to be doped and their electronic structures are greatly modified by the organic molecules, providing a promising method to tailor the electronic and transport properties of graphene-based devices.[12−14] Meanwhile, the molecule–graphene interaction also plays a key role in the molecular self-assembly on graphene, since the final self-assembly is essentially governed by the subtle balance between molecule–substrate and molecule–molecule interactions.[15,16]

Metal phthalocyanine molecules (MPcs), each consisting of a central metal ion and a macrocycle of alternating carbon and nitrogen atoms (Figure 1a), have been attracting considerable interest because of their potential applications in organic electronic and spintronic devices.[17−20] Formation of densely packed monolayer on graphite,[21−23] NaCl,[24,25] Au(111),[26,27] Ag(111),[28,29] and Cu(111)[25,30] surfaces and Kagome lattice on metal surfaces[31,32] was revealed by various scanning tunneling microscopy (STM) studies. Recently, we adopted the moiré pattern of monolayer graphene (MG) that originates from the lattice mismatch between MG and Ru(0001) surface as a template and fabricated regular Kagome lattices of MPcs.[16] We revealed that the site-specific anchoring of FePc molecules on the moiré pattern of MG/Ru(0001) is driven by the lateral

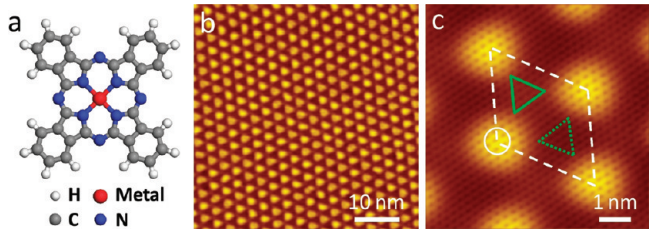

Figure 1. (a) Chemical structure of MPc molecules. (b) Large-scale STM image of graphene grown on Ru(0001), showing the hexagonal moiré pattern due to the lattice mismatch between graphene and Ru substrate. (c) Zoom-in STM image with atomic resolution, showing the unit cell of the moiré pattern. Atop, fcc, and hcp regions are indicated by the circle, solid triangle, and dashed triangle, respectively. Scanning parameters: (b) sample bias $U = -1$ V, tunneling current $I =$ 0.03 nA; (c) U = −0.2 V, $I = 0.5$ nA.

Received: April 27, 2012
Revised: June 1, 2012
Published: June 2, 2012

dx.doi.org/10.1021/jp304068a | J. Phys. Chem. C 2012, 116, 14052−14056

dipole field of MG/Ru(0001).[15] However, a comparative investigation of the self-assembly of a series of MPc molecules on MG/Ru(0001) is still missing, which might be very helpful for understanding the interfacial coupling between MPc molecules and MG/Ru(0001).

In this article, we present the self-assembly of a series of MPc molecules on MG/Ru(0001) and MG/Pt(111) for comparison by means of LT-STM. Formation of dispersive single molecules, dispersive molecular chains, and small patches of Kagome lattice are observed for FePc, MnPc, NiPc, and H_2Pc on graphene/Ru(0001), respectively, at low coverage. In contrast, although the MG/Pt(111) exhibits various domains with different moiré patterns and corrugations, FePc molecules always form densely packed two-dimensional islands with a square lattice on MG/Pt(111) at submonolayer coverage. From these different self-assembling behaviors the strength of molecule−substrate interactions is compared for MPc molecules on MG/Ru(0001) and MG/Pt(111).

EXPERIMENTAL SECTION

Our experiments were carried out in two separate ultra-high-vacuum (base pressure of 1×10^{-10} mbar) LT-STM systems (Unisoku and Omicron) equipped with standard surface preparation facilities. Ru(0001) and Pt(111) (Mateck, Germany) surfaces were prepared by repeated cycles of Ar^+ sputtering and annealing at 950 and 900 °C, respectively. High-quality and large area MG was obtained via pyrolysis of ethylene on Ru(0001) and Pt(111), as described elsewhere.[9,33] Commercial FePc, MnPc, NiPc, and H_2Pc molecules (Sigma-Aldrich, 97% purity) were purified via vacuum sublimation before deposition. MPc molecules were deposited via vacuum sublimation from two Knudsen-type evaporators, while MG/Ru(0001) or MG/Pt(111) substrates were held at room temperature (RT). One monolayer (ML) refers to completion of a close-packed MPc layer on MG/Ru(0001) or MG/Pt(111) surfaces, as estimated with STM. STM images were acquired in constant-current mode, and all given voltages refer to the sample. All experiments were performed with electrochemically etched tungsten tips at 4.2 K.

RESULTS AND DISCUSSION

The as-prepared MG on Ru(0001) shows a regular moiré pattern with a periodicity of ∼3 nm (Figure 1b) due to the lattice mismatch between MG and Ru(0001) surface. Three different regions, namely, atop, fcc, and hcp regions, can be distinguished in each unit cell of the MG moiré pattern (Figure 1c) according to the stacking of the carbon atoms of MG with respect to the Ru(0001) surface.[9] These different regions show different apparent heights due to the geometrical corrugation of MG. Moreover, they exhibit very different local electronic structures, such as image potential states and work functions,[34] which can dramatically influence the self-assembling behavior of organic molecules.[15]

Figure 2 shows the STM images after deposition of ∼0.15 ML MPc molecules on MG/Ru(0001) surface. Each MPc molecule exhibits a cross structure, except that the center of the cross is either a bright protrusion or a depression, depending on the central metal ions of the MPc molecules. For FePc and MnPc (Figure 2a and 2b), the molecular center shows a pronounced protrusion, which originates from the d_{z^2} orbitals of the central metal ions of Fe^{2+} or Mn^{2+}.[27] The four dim lobes surrounding the central protrusion are assigned to the four

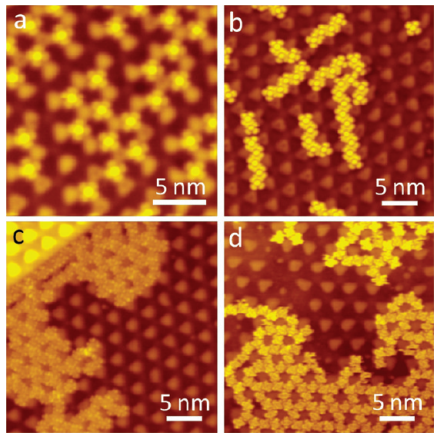

Figure 2. STM images obtained after deposition of ∼0.15 ML MPc molecules on MG/Ru(0001), showing different self-assembling behaviors. (a) Dispersive individual FePc molecules at fcc regions. (b) Molecular chains of MnPc at fcc and hcp regions. (c and d) Small patches of Kagome lattice of NiPc and H_2Pc, respectively. Scanning parameters: (a) $U = -2$ V, $I = 2$ pA, (b) $U = -1$ V, $I = 6$ pA, (c) $U = -2$ V, $I = 1$ pA, (d) $U = -1$ V, $I = 50$ pA.

benzene rings of the MPc molecules. For NiPc and H_2Pc (Figure 2c and 2d), the cross centers show depressions with respect to the four lobes, in line with previous reports for NiPc and H_2Pc adsorbed on metal substrates.[27,29] However, the self-assembling behavior of the MPc molecules on MG/Ru(0001) are remarkably different, despite their similar molecular structures and cross-shaped features in STM images. As seen in Figure 2a, FePc molecules are exclusively accommodated at the fcc regions of the MG moiré pattern. In contrast, MnPc molecules occupy both fcc and hcp regions of the MG moiré pattern and form molecular chains with variable lengths, as seen in Figure 2b. These molecular chains, however, are dispersive without forming extended two-dimensional (2D) molecular aggregations. Instead, NiPc molecules indiscriminately occupy the two relatively low regions (fcc and hcp regions) of the MG moiré pattern and form small patches of Kagome lattice, as shown in Figure 2c. A similar behavior is also observed for H_2Pc adsorption on MG/Ru(0001) (Figure 2d). Previous experiments and theoretical calculations show that the charge transfer from Ru(0001) substrate to MG is strongly spatial dependent, which results in the inhomogeneous electronic structures of the atop, fcc, and hcp regions of the MG moiré pattern.[15] The local work function of the fcc and hcp region is ∼0.2 and ∼0.25 eV lower than that of the atop region,[15] respectively. This explains the preferential occupation of the fcc and hcp regions by MnPc, NiPc, and H_2Pc molecules. Nevertheless, for FePc, the variation of the local work function is inconsistent with the observed preferential occupation. In fact, theoretical calculations reveal that their exclusive accommodation at the fcc regions is driven by the lateral electric (dipole) field.[15]

The different self-assembling behavior of FePc, MnPc, NiPc, and H_2Pc molecules on MG/Ru(0001) at the initial stage clearly show that a delicate balance between the molecule−molecule interaction and the molecule−substrate interaction governs the supramolecular self-assembly. In general, when there is a significant lattice mismatch between the molecular adlayer and the substrate, the domination of molecule−molecule interaction over molecule−substrate interaction favors formation of extended 2D molecular aggregations with

dx.doi.org/10.1021/jp304068a | J. Phys. Chem. C 2012, 116, 14052−14056

an intermolecular distance close to that of the molecular adlayer, whereas the domination of molecule−substrate interaction over molecule−molecule interaction tends to drive a selective adsorption of the molecules at the specific sites of the substrate with lowest total energy. The fact that FePc molecules exclusively occupy the fcc regions of the MG moiré pattern indicates that the molecule−substrate interaction dominates over the molecule−molecule interaction for FePc molecules self-assembling on MG/Ru(0001). Meanwhile, formation of small patches of Kagome lattice for NiPc and H_2Pc molecules adsorption on MG/Ru(0001) shows that the molecule−molecule interaction dominates over the molecule−substrate interaction at the fcc and hcp regions of the MG moiré pattern. For MnPc, the intermediate self-assembling behavior in between that of FePc and NiPc suggests that the molecule−molecule and molecule−substrate interactions might be comparable. Since the MPc molecules have similar molecular skeletons, a similar intermolecular coupling is expected for various MPc molecules self-assembling on MG/Ru(0001). Thus, the different self-assembling behavior of FePc, MnPc, NiPc, and H_2Pc molecules on MG/Ru(0001) evidences that the molecule−substrate interactions for different MPc molecules decrease in the sequence of FePc > MnPc > NiPc and H_2Pc. Recently, Dou and co-workers studied the molecule−substrate interaction channels of a variety of MPcs on MG/Ni(111) surface by means of high-resolution electron energy loss spectroscopy and reported that the molecule−substrate interaction is quite weak and comparable with the $\pi-\pi$ interaction between molecules in the case of NiPc, whereas it is much stronger in the case of FePc,[35] in line with our results. We note that the molecule−substrate interaction is rather weak even for the strongest coupling between FePc and MG/Ru(0001), as FePc molecules can be frequently displaced by the STM tip during scanning with normal parameters (e.g., sample bias $U = -1.0$ V, tunneling current $I = 0.2$ nA).

We managed to directly compare the molecule−substrate coupling for FePc and H_2Pc via codeposition of these two species on MG/Ru(0001). In a first step, we deposit ∼0.75 ML H_2Pc molecules on MG/Ru(0001) and prepare a highly ordered Kagome lattice of H_2Pc.[16] Then, FePc molecules are deposited on the as-prepared H_2Pc Kagome lattice on MG/Ru(0001). Figure 3a shows the STM image after addition of ∼0.05 ML FePc molecules on the as-prepared H_2Pc Kagome lattice on MG/Ru(0001). A selective trapping of FePc molecules at the pores of the H_2Pc Kagome lattice is not observed, in contrast to formation of a host−guest complex of FePc or *tert*-butyl zinc phthalocyanine ($(t\text{-Bu})_4$−ZnPc) on FePc Kagome lattice.[36] Instead, some H_2Pc molecules of the Kagome lattice are replaced by FePc molecules, leading to formation of a bicomponent Kagome lattice with significant distortion (Figure 3b). This behavior indicates that the interaction between FePc and MG/Ru(0001) at the fcc regions is stronger than that between H_2Pc and MG/Ru(0001). At a FePc coverage of ∼0.25 ML, a complete close-packed adlayer with a square lattice is formed, as shown in Figure 3c and 3d. This adlayer consists of FePc and H_2Pc molecules, and a corrugation stemmed from the MG moiré pattern is clearly visible. It is noteworthy that all FePc molecules are located at the fcc and hcp regions of the MG moiré pattern, and none is at the atop region, further confirming a stronger molecule−substrate interaction for FePc than that for H_2Pc.

It was reported that the organic molecules can be electronically decoupled from metal substrates by MG that is

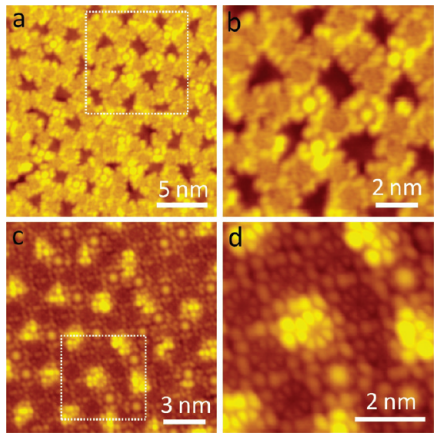

Figure 3. (a) STM images after addition of ∼0.05 ML FePc molecules on the as-prepared H_2Pc Kagome lattice on MG/Ru(0001). (b) Zoom-in STM image showing the bicomponent Kagome lattice resulting from substitution of several H_2Pc with FePc. Note that the FePc molecules show bright protrusions at the molecular center, while the center of a H_2Pc molecule is imaged as a depression. (c and d) STM images after increasing FePc coverage to ∼0.25 ML, showing a complete close-packed square lattice. Scanning parameters: (a and b) $U = -3$ V, $I = 30$ pA; (c and d) $U = -2.5$ V, $I = 50$ pA.

grown on the metal substrates.[37] Nevertheless, the Ru(0001) substrate still plays an important role in the molecule−substrate interaction for MPc molecules on MG/Ru(0001). In order to understand how the metal substrates influence the molecule−substrate interaction for MPc molecules on MG, it is desirable to compare the self-assembly of MPc molecules on MG/Pt(111). The reason for choosing MG/Pt(111) lies in the fact that MG grown on Pt(111) exhibits various domains with different moiré superstructures, such as the rippled ones of $(\sqrt{37} \times \sqrt{37})$ R21°, $(\sqrt{61} \times \sqrt{61})$ R26°, and $(\sqrt{67} \times \sqrt{67})$ R12° and the unrippled ones of 2 × 2, 3 × 3, and 4 × 4 with respect to the Pt(111) surface,[38] in contrast to the cases of corrugated MG grown on Ru(0001) and flat MG grown on Ni(111).[8] Since the coupling between FePc molecules and substrates of either MG/Ru(0001) or MG/Ni(111) is the strongest among various MPc molecules,[35] we focus on the self-assembly of FePc on MG/Pt(111).

Figure 4a shows a large-scale STM image after deposition of ∼0.3 ML FePc on MG/Pt(111) at RT. Formation of two ordered close-packed islands of FePc is clearly seen, indicating the domination of molecule−molecule interaction over molecule−substrate interaction. The traces between these two molecular islands are assigned to mobile FePc molecules, which are in a 2D fluid phase. This 2D fluid phase is in dynamic equilibrium with the ordered FePc inlands, leading to fluctuation of the island edges. These behaviors also suggest a weak bonding between FePc molecules and graphene. The zoom-in STM image of one of the FePc islands (Figure 4b) reveals a square lattice with a lattice constant of about 1.38 nm, akin to that of FePc monolayer grown on MG/Ru(0001).[36] To figure out the impact of MG moiré superstructures upon the self-assembling behavior of FePc molecules, we carefully acquire high-resolution STM images on the MG regions (Figure 4c and 4d) very close to several close-packed islands of FePc. We find that FePc molecules can form close-packed islands on any type of MG moiré superstructure on Pt(111). Hence, the MG moiré superstructures, either rippled or

dx.doi.org/10.1021/jp304068a | J. Phys. Chem. C 2012, 116, 14052−14056

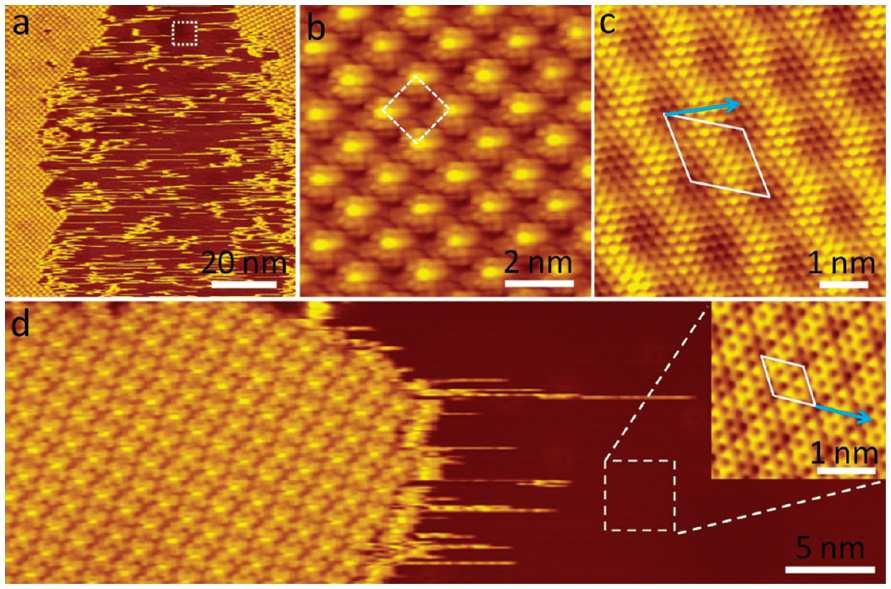

Figure 4. STM image after deposition of ~0.3 ML FePc on MG/Pt(111). (a) Large-scale image showing formation of close-packed molecule islands. (b) Zoom-in STM image of a closed-packed FePc molecular island in a showing a square lattice (indicated by the dashed square). (c) High-resolution STM image of the MG region indicated by the dashed square in a, showing a $(\sqrt{37} \times \sqrt{37})$ R21° moiré superstructure with respect to the primary graphene lattice. ⟨11−20⟩ direction of graphene lattice is indicated by the blue arrow and moiré unit cell by the white rhombus. (d) STM image of another molecular island. (Inset) Close-up of the MG region close to the island with a 3 × 3 moiré supercell with respect to graphene. Scanning parameters: (a) $U = -0.2$ V, $I = 10$ pA, (b) $U = -0.4$ V, $I = 10$ pA, (c) $U = -10$ mV, $I = 0.1$ nA, (d) $U = -0.2$ V, $I = 20$ pA, (inset) $U = -40$ mV, $I = 80$ pA.

unrippled, show no significant effect on the self-assembly of FePc on MG/Pt(111).

Considering a similar molecule−molecule interaction in both cases, our experiments reveal that the molecule−substrate interaction for FePc on MG/Ru(0001) is stronger than that for FePc on MG/Pt(111). This can be rationalized by the different coupling between MG and metal substrates. Our DFT calculations show that the interaction between MG and Pt(111) is rather weak for either rippled or unrippled moiré superstructures and the MG is quasi-free-standing.[38] The free electrons of MG are confined in the plane of MG due to the sp^2 bonds between C atoms. Thus, the free electrons cannot be efficiently coupled with the molecular orbitals of MPc adsorbates. Meanwhile, in the case of MG grown on Ru(0001), MG is strongly coupled with Ru(0001) substrate at the fcc and hcp regions of the MG moiré pattern, leading to a remarkable charge transfer from Ru(0001) substrate to MG at these regions.[15] This inhomogeneous charge redistribution not only dopes MG but also modifies the C−C bonds of MG from a nearly pure sp^2 to partial sp^3 characteristic,[39,40] which is more extended from the MG surface and favors a stronger coupling with molecular orbitals of MPc adsorbates. Moreover, the lateral electric field also contributes to the strong binding between MPc molecules and MG/Ru(0001) substrate.[15]

CONCLUSIONS

We investigated the self-assembly of a family of MPc molecules on MG/Ru(0001) and MG/Pt(111) by means of LT-STM. At low coverage, dispersive single molecules, dispersive molecular chains, and small patches of Kagome lattice are observed for FePc, MnPc, NiPc, and H_2Pc on MG/Ru(0001). In contrast, although MG/Pt(111) exhibits various domains with different moiré patterns and corrugations, FePc molecules always form densely packed 2D islands with a square lattice on MG/Pt(111) at submonolayer coverage. From the different self-assembling behavior of MPc molecules on MG/Ru(0001), we propose that the molecule−substrate interactions decrease in the sequence of FePc > MnPc > NiPc and H_2Pc for MPc molecules on MG/Ru(0001). The molecule−substrate interaction for FePc on MG/Ru(0001) is stronger than that for FePc on MG/Pt(111). This work about the self-assembling behavior and molecule−substrate coupling of various MPc molecules on MG/Ru(0001) and MG/Pt(111) is helpful for a comprehensive understanding and control of the structural and physical properties of the MPc molecules on graphene surfaces at the single molecular level.

AUTHOR INFORMATION

Corresponding Author

*Phone: +86-10-82648035. Fax: +86-10-62556598. E-mail: hjgao@iphy.ac.cn.

Notes

The authors declare no competing financial interest.

ACKNOWLEDGMENTS

Financial support from the NNSFC (20973196), National "973" project (2009CB929103 and 2010CB923004) of China, and CAS is gratefully acknowledged.

REFERENCES

(1) Novoselov, K. S.; Geim, A. K.; Morozov, S. V.; Jiang, D.; Zhang, Y.; Dubonos, S. V.; Grigorieva, I. V.; Firsov, A. A. *Science* **2004**, *306*, 666−669.

(2) Novoselov, K. S.; Geim, A. K.; Morozov, S. V.; Jiang, D.; Katsnelson, M. I.; Grigorieva, I. V.; Dubonos, S. V.; Firsov, A. A. *Nature* **2005**, *438*, 197−200.

(3) Zhang, Y.; Tan, Y.-W.; Stormer, H. L.; Kim, P. *Nature* **2005**, *438*, 201−204.

(4) Bae, S.; Kim, H.; Lee, Y.; Xu, X.; Park, J.-S.; Zheng, Y.; Balakrishnan, J.; Lei, T.; Ri Kim, H.; Song, Y. I.; et al. *Nat. Nanotechnol.* **2010**, *5*, 574−578.
(5) Liu, M.; Yin, X.; Ulin-Avila, E.; Geng, B.; Zentgraf, T.; Ju, L.; Wang, F.; Zhang, X. *Nature* **2011**, *474*, 64−67.
(6) Lin, Y.-M.; Valdes-Garcia, A.; Han, S.-J.; Farmer, D. B.; Meric, I.; Sun, Y.; Wu, Y.; Dimitrakopoulos, C.; Grill, A.; Avouris, P.; et al. *Science* **2011**, *332*, 1294−1297.
(7) Park, J.-U.; Nam, S.; Lee, M.-S.; Lieber, C. M. *Nat. Mater.* **2012**, *11*, 120−125.
(8) Gao, M.; Pan, Y.; Zhang, C. D.; Hu, H.; Yang, R.; Lu, H. L.; Cai, J. M.; Du, S. X.; Liu, F.; Gao, H.-J. *Appl. Phys. Lett.* **2010**, *96*, 053109.
(9) Pan, Y.; Zhang, H. G.; Shi, D. X.; Sun, J. T.; Du, S. X.; Liu, F.; Gao, H.-J. *Adv. Mater.* **2009**, *21*, 2777−2780.
(10) Murata, Y.; Petrova, V.; Kappes, B. B.; Ebnonnasir, A.; Petrov, I.; Xie, Y.-H.; Ciobanu, C. V.; Kodambaka, S. *ACS Nano* **2010**, *4*, 6509−6514.
(11) Ugeda, M. M.; Fernández-Torre, D.; Brihuega, I.; Pou, P.; Martínez-Galera, A. J.; Pérez, R.; Gómez-Rodríguez, J. M. *Phys. Rev. Lett.* **2011**, *107*, 116803.
(12) Chen, W.; Chen, S.; Qi, D. C.; Gao, X. Y.; Wee, A. T. S. *J. Am. Chem. Soc.* **2007**, *129*, 10418−10422.
(13) Dong, X.; Fu, D.; Fang, W.; Shi, Y.; Chen, P.; Li, L.-J. *Small* **2009**, *5*, 1422−1426.
(14) Zhang, Z.; Huang, H.; Yang, X.; Zang, L. *J. Phys. Chem. Lett.* **2011**, *2*, 2897−2905.
(15) Zhang, H. G.; Sun, J. T.; Low, T.; Zhang, L. Z.; Pan, Y.; Liu, Q.; Mao, J. H.; Zhou, H. T.; Guo, H. M.; Du, S. X.; et al. *Phys. Rev. B* **2011**, *84*, 245436.
(16) Mao, J. H.; Zhang, H. G.; Jiang, Y. H.; Pan, Y.; Gao, M.; Xiao, W. D.; Gao, H.-J. *J. Am. Chem. Soc.* **2009**, *131*, 14136−14137.
(17) Gao, L.; Ji, W.; Hu, Y. B.; Cheng, Z. H.; Deng, Z. T.; Liu, Q.; Jiang, N.; Lin, X.; Guo, W.; Du, S. X.; et al. *Phys. Rev. Lett.* **2007**, *99*, 106402.
(18) Gao, H.-J.; Gao, L. *Prog. Surf. Sci.* **2010**, *85*, 28−91.
(19) Tsukahara, N.; Noto, K.-i.; Ohara, M.; Shiraki, S.; Takagi, N.; Takata, Y.; Miyawaki, J.; Taguchi, M.; Chainani, A.; Shin, S.; et al. *Phys. Rev. Lett.* **2009**, *102*, 167203.
(20) Zhao, A.; Li, Q.; Chen, L.; Xiang, H.; Wang, W.; Pan, S.; Wang, B.; Xiao, X.; Yang, J.; Hou, J. G.; et al. *Science* **2005**, *309*, 1542−1544.
(21) Åhlund, J.; Schnadt, J.; Nilson, K.; Göthelid, E.; Schiessling, J.; Besenbacher, F.; Mårtensson, N.; Puglia, C. *Surf. Sci.* **2007**, *601*, 3661−3667.
(22) Gopakumar, T. G.; Lackinger, M.; Hackert, M.; Müller, F.; Hietschold, M. *J. Phys. Chem. B* **2004**, *108*, 7839−7843.
(23) Nilson, K.; Ahlund, J.; Brena, B.; Gothelid, E.; Schiessling, J.; Martensson, N.; Puglia, C. *J. Phys. Chem.* **2007**, *127*, 114702.
(24) Wang, Y.; Kröger, J. r.; Berndt, R.; Tang, H. *J. Am. Chem. Soc.* **2010**, *132*, 12546−12547.
(25) Scarfato, A.; Chang, S.-H.; Kuck, S.; Brede, J.; Hoffmann, G.; Wiesendanger, R. *Surf. Sci.* **2008**, *602*, 677−683.
(26) Cheng, Z. H.; Gao, L.; Deng, Z. T.; Liu, Q.; Jiang, N.; Lin, X.; He, X. B.; Du, S. X.; Gao, H.-J. *J. Phys. Chem. C* **2007**, *111*, 2656−2660.
(27) Lu, X.; Hipps, K. W. *J. Phys. Chem. B* **1997**, *101*, 5391−5396.
(28) Wang, Y.; Kröger, J.; Berndt, R.; Hofer, W. *Angew. Chem., Int. Ed.* **2009**, *48*, 1261−1265.
(29) Bai, Y.; Buchner, F.; Wendahl, M. T.; Kellner, I.; Bayer, A.; Steinruck, H.-P.; Marbach, H.; Gottfried, J. M. *J. Phys. Chem. C* **2008**, *112*, 6087−6092.
(30) Karacuban, H.; Lange, M.; Schaffert, J.; Weingart, O.; Wagner, T.; Möller, R. *Surf. Sci.* **2009**, *603*, L39−L43.
(31) Shi, Z.; Lin, N. *J. Am. Chem. Soc.* **2009**, *131*, 5376−5377.
(32) Wang, Y.; Ge, X.; Manzano, C.; Kröger, J. r.; Berndt, R.; Hofer, W. A.; Tang, H.; Cerda, J. *J. Am. Chem. Soc.* **2009**, *131*, 10400−10402.
(33) Pan, Y.; Shi, D. X.; Gao, H.-J. *Chin. Phys* **2007**, *16*, 3151−3153.
(34) Zhang, H. G.; Hu, H.; Pan, Y.; Mao, J. H.; Gao, M.; Guo, H. M.; Du, S. X.; Greber, T.; Gao, H.-J. *J. Phys.: Condens. Matter* **2010**, *22*, 302001.
(35) Dou, W.; Huang, S.; Zhang, R. Q.; Lee, C. S. *J. Phys. Chem.* **2011**, *134*, 094705.
(36) Zhang, H. G.; Xiao, W. D.; Mao, J. H.; Zhou, H. T.; Li, G.; Zhang, Y.; Du, S. X.; Gao, H.-J. *J. Phys. Chem. C* **2012**, *116*, 11091−11095.
(37) Zhou, H. T.; Mao, J. H.; Li, G.; Wang, Y. L.; Feng, X. L.; Du, S. X.; Mullen, K.; Gao, H.-J. *Appl. Phys. Lett.* **2011**, *99*, 153101.
(38) Gao, M.; Pan, Y.; Huang, L.; Hu, H.; Zhang, L. Z.; Guo, H. M.; Du, S. X.; Gao, H.-J. *Appl. Phys. Lett.* **2011**, *98*, 033101.
(39) Feibelman, P. J. *Phys. Rev. B* **2008**, *77*, 165419.
(40) Pan, Y.; Gao, M.; Huang, L.; Liu, F.; Gao, H.-J. *Appl. Phys. Lett.* **2009**, *95*, 093106.